Pseudogap formation in an electronic system with *d*-wave attraction at low density

Takashi Hotta, Matthias Mayr, and Elbio Dagotto

National High Magnetic Field Laboratory, Florida State University, Tallahassee, Florida 32306

On the basis of an electronic model with separable attractive interaction, the precursors at high temperature and strong coupling of the *d*-wave superconducting state are investigated in the one-particle spectral function $A(\mathbf{k}, \omega)$ and the total density of states $\rho(\omega)$, with the use of the self-consistent *t*-matrix approximation. In the low-density region, it is found that a gaplike structure at the Fermi level appears in $A(\mathbf{k}, \omega)$ and $\rho(\omega)$ above the superconducting transition temperature. It is shown that the pseudogap energy scale is determined by the binding energy of the Cooper pair. [S0163-1829(99)00142-3]

I. INTRODUCTION

In the underdoped high-T_c superconductors (HTSC), pseudogap (PG) behavior has been widely observed in experiments such as NMR,[1] specific heat,[2] and photoemission.[3] All these phenomena can be basically understood as caused by the suppression of low-energy spectral weight in the temperature range $T_c \lesssim T \lesssim \Delta_{\mathrm{PG}}$, where T_c is the superconducting transition temperature and Δ_{PG} is a characteristic energy scale for the PG formation. This occurs both in the spin- and charge-excitation spectra. As a consequence, the problem is reduced to the clarification of the origin of this spectral-weight suppression, namely, the physical origin of Δ_{PG}.

The angle-resolved photoemission (ARPES) spectrum, which is sensitive to the momentum dependence of the PG, has revealed that the PG phenomenon itself exhibits a *d*-wave symmetry which is smoothly connected to the *d*-wave superconducting gap.[3] Moreover, the locus of the minimum gap position in momentum space traces the shape of the Fermi surface. From these results, it can be inferred that the energy scale for PG formation is closely related to the superconducting correlation. Then, one of the possible explanations for the PG behavior involves the discussion of possible ''precursors'' of the Cooper-pair formation above T_c. Certainly there are other possible scenarios that also lead to PG formation such as spinon pairing,[4] antiferromagnetic (AF) spin fluctuation,[5] and fermion-boson model,[6] but in this paper the focus will be precisely on the development of a PG at strong coupling due to the formation of electron bound states at a temperature scale larger than the one corresponding to long-range superconducting pairing.

Along this scenario, much effort has been devoted to the investigation of the PG phenomena.[7–24] However, there are few results in the literature leading to PG with *d*-wave symmetry, while the PG in the *s*-wave superconductor has been intensively investigated on the basis of the negative-*U* Hubbard model. The popularity of the *s*-wave calculations as opposed to the more realistic *d*-wave case is mainly due to technical issues. The quantum Monte Carlo (QMC) simulation provides accurate information on the negative-*U* Hubbard model and with these results the validity of other diagrammatic method such as the self-consistent *t*-matrix approximation (SCTMA) can be checked. However, for the model with *d*-wave attraction (or the nearest-neighbor attrac-

tion), QMC calculations are difficult mainly due to sign problems in the simulations and also because phase separation could occur for a model with an attractive potential that acts at finite distances, contrary to what occurs in the attractive Hubbard model where the attraction is only on site.[25]

In spite of these potential difficulties, here the *d*-wave PG is studied in order to contribute to the investigation of the energy scale Δ_{PG} in HTSC. For this purpose, here an effective model with *d*-wave separable attraction is analyzed, focusing our efforts into the low-density regime, for the following reasons. First, from a physical point of view, the low carrier density region is important because the underdoped HTSC regime as a first approximation can be described as a low-density gas of holes in an AF background. Previous numerical studies have shown that holes in such an environment behave like quasiparticles with a bandwidth renormalized to be of order J, the Heisenberg exchange coupling.[26] Second, now from a technical viewpoint, it is known that the SCTMA gives reliable results in the dilute limit.[27] Then, the behavior of the spectral function can be safely investigated in the low-density region. For these reasons in the present paper the average electron filling will actually be at most 10%. Note that our ''electrons'' below will simply represent fermions interacting through an attractive potential, and thus they can be thought of as ''holes'' in the context of HTSC.

As mentioned before, the preformed *s*-wave pairing features in the negative-*U* Hubbard model have been widely investigated as a prototype for PG formation in the underdoped HTSC. Besides the technical aspects already discussed, this seems to be based on the assumption that the difference *s* vs *d* in the pairing symmetry does not play an essential role in the PG formation. This may seem correct by observing the gaplike structure in the total density of states (TDOS), because it appears around the Fermi level irrespective of the pairing symmetry, although the actual detailed shape is different. However, recalling that the main features for the PG formation in the underdoped HTSC have been revealed using ARPES technique, the structure in the individual one-particle spectral function should play a crucial role. In fact, important differences between *s*- and *d*-wave symmetry fairly clearly appear in the spectral function described below in our study.

In this paper, it is reported that the Δ_{PG} scale agrees with the binding energy of the Cooper pair irrespective of the

pairing symmetry. The main difference between *s*- and *d*-wave symmetry, appears in the momenta of preformed-pair electrons $\mathbf{K}$ and $-\mathbf{K}$. For the *s*-wave symmetry, $\mathbf{K}$ is always determined by the band structure. Namely, in the dilute limit, it is given by the momentum at the bottom of the band, $\mathbf{k}^*$. Since the attraction is uniform in momentum space, $\mathbf{K}$ is determined only by the kinetic energy for the *s*-wave case. On the other hand, for a strong attraction with *d*-wave symmetry, $\mathbf{K}$ is not given by $\mathbf{k}^*$, but is located at $(\pi,0)$ and $(0,\pi)$, because the attraction becomes maximum at those momenta. Such a competition between the band structure and the strong attractive interaction leads to interesting features in the *d*-wave PG, while the *s*-wave PG simply follows the band structure.

This paper is organized as follows. In Sec. II, a general formalism to calculate the electronic self-energy in the SCTMA on the real-frequency axis is present. For the investigation of the PG structure for the *d*-wave attraction, a technical trick called ''the *s*-*d* conversion'' is introduced. Section III is devoted to the results obtained with the formalism of Sec. II. Two types of band structures are considered with $\mathbf{k}^*=(0,0)$ and $(\pi,0)$, respectively. In Sec. IV, the results are discussed. Finally in Sec. V, after providing some comments, the main results of this paper are summarized. Throughout this paper, units such that $\hbar=k_B=1$ are used.

II. FORMULATION

A. Hamiltonian

Let us consider a simple model in which electrons are coupled with each other through a separable attractive interaction. The symmetry of the electron pair is contained in the attractive term of the model, but it is not necessary to write it explicitly in most of the formulation of this section, although it will become important for the discussion on the PG. The model Hamiltonian is written as

$$H=\sum_{\mathbf{k}\sigma}(\varepsilon_\mathbf{k}-\mu)c^\dagger_{\mathbf{k}\sigma}c_{\mathbf{k}\sigma}+\sum_{\mathbf{k},\mathbf{k}',\mathbf{q}}V_{\mathbf{k}'-\mathbf{k}}c^\dagger_{\mathbf{k}\uparrow}c^\dagger_{\mathbf{q}-\mathbf{k}\downarrow}c_{\mathbf{q}-\mathbf{k}'\downarrow}c_{\mathbf{k}'\uparrow},$$
(2.1)

where $c_{\mathbf{k}\sigma}$ is the annihilation operator for an electron with momentum $\mathbf{k}$ and spin σ, $\varepsilon_\mathbf{k}$ the one-electron energy, μ the chemical potential, and $V_{\mathbf{k},\mathbf{k}'}$ the pair interaction between electrons. The electron dispersion is expressed as

$$\varepsilon_\mathbf{k}=-2t(\cos k_x+\cos k_y)-4t'\cos k_x\cos k_y,\quad (2.2)$$

where t and t' are the nearest and next-nearest neighbor hopping amplitudes, respectively. The pair interaction is written as

$$V_{\mathbf{k}'-\mathbf{k}}=-Vf_\mathbf{k}f_{\mathbf{k}'},\qquad (2.3)$$

where $f_\mathbf{k}$ is the form factor with $f_{-\mathbf{k}}=f_\mathbf{k}$ characterizing the symmetry of the singlet Cooper pair. Note that a positive value of V denotes an attractive interaction throughout this paper.

It may be argued that the above separable-type attraction is only an artificial interaction. This criticism is reasonable, since the purely separable potential is not realized in real materials. However, the present interaction is a portion of the nearest-neighbor attractive interaction, which is a more real-
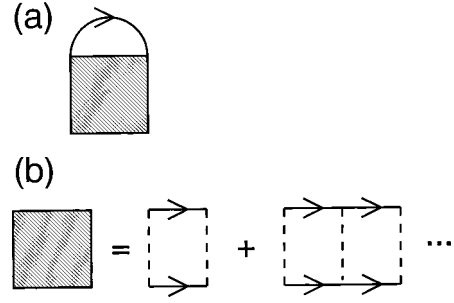

FIG. 1. (a) Self-energy in the SCTMA. The hatched square and the solid line denote the *t*-matrix Γ and the renormalized Green's function G, respectively. (b) Diagrammatic representation for Γ. The broken lines indicate the interaction.

istic model for *d*-wave superconductivity.[26] In addition, our purpose in this work is to clarify the energy scale for the *d*-wave PG in the normal state, not to make a quantitative comparison with the experimental results observed in HTSC. Thus it is reasonable to investigate first the simplest electronic model which certainly shows the *d*-wave superconducting ground state, postponing for the future the analysis of more realistic models.

B. Self-consistent *t*-matrix approximation

Now let us calculate the spectral function using the SCTMA. Since this method becomes exact in the two-particle problem, it is expected to give a reliable result in the low-density region.[27] In fact, this expectation has been already checked in the attractive Hubbard model by comparing SCTMA results against QMC simulations.[28] Therefore the reliability of the SCTMA may also be expected for the non-*s*-wave attractive interaction, even though the direct comparison with QMC results is quite difficult in this case.

Consider first for completeness the imaginary-axis representation. In this formulation, the one-particle Green's function G is given by

$$G(\mathbf{k},i\omega_n)=\frac{1}{i\omega_n-(\varepsilon_\mathbf{k}-\mu)-\Sigma(\mathbf{k},i\omega_n)},\qquad (2.4)$$

where $\omega_n=\pi T(2n+1)$, n is an integer, and T the temperature. In the SCTMA, the self-energy $\Sigma(\mathbf{k},i\omega_n)$ is obtained with the use of the *t* matrix given by the infinite sum of particle-particle (p-p) ladder diagrams, as shown in Fig. 1. More explicitly, Σ is expressed as

$$\Sigma(\mathbf{k},i\omega_n)=f_\mathbf{k}^2\ T\sum_{n'}\ \sum_{\mathbf{k}'}\Gamma(\mathbf{k}+\mathbf{k}',i\omega_n+i\omega_{n'})$$
$$\times G(\mathbf{k}',i\omega_{n'}),\qquad (2.5)$$

where $\Gamma(\mathbf{q},i\nu_m)$ is the *t* matrix, given by

$$\Gamma(\mathbf{q},i\nu_m)=\frac{-V^2\phi(\mathbf{q},i\nu_m)}{1-V\phi(\mathbf{q},i\nu_m)}.\qquad (2.6)$$

Here $\nu_m=2\pi Tm$, with m an integer, and $\phi(\mathbf{q},i\nu_m)$ is the p-p ladder, defined by

$$\phi(\mathbf{q}, i\nu_m) = T\sum_n \sum_{\mathbf{k}} f_{\mathbf{k}}^2 G(\mathbf{k}, i\omega_n) G(\mathbf{q}-\mathbf{k}, i\nu_m - i\omega_n).$$

$$(2.7)$$

Note that the Hartree term is neglected in the self-energy because it should be considered as included in the band structure. The Green's function can be calculated self-consistently using Eqs. (2.4)–(2.7). The chemical potential is determined by

$$\langle n \rangle/2 = T\sum_n \sum_{\mathbf{k}} e^{i\omega_n \eta} G(\mathbf{k}, i\omega_n),   (2.8)$$

where $\langle n \rangle$ is the average electron number density per site and η is an infinitesimal positive number. In order to obtain results on the real-frequency axis, Padé approximants for the numerical analytic continuation from the imaginary-axis data are frequently used.[29] However, in general, it is difficult to control the accuracy of the calculation by this procedure.

In this paper, our efforts are focused on the direct calculation of the Green's function on the real-frequency axis.[19] In this context, a self-consistent calculation for the spectral function

$$A(\mathbf{k}, \omega) = (-1/\pi) \operatorname{Im} G(\mathbf{k}, \omega),   (2.9)$$

is carried out, where the retarded Green's function $G(\mathbf{k}, \omega)$ is given by

$$G(\mathbf{k}, \omega) = \frac{1}{\omega - (\varepsilon_{\mathbf{k}} - \mu) - \Sigma(\mathbf{k}, \omega)}.   (2.10)$$

The imaginary part of the retarded self-energy is expressed as

$$\operatorname{Im}\Sigma(\mathbf{k}, \omega) = f_{\mathbf{k}}^2 \sum_{\mathbf{k}'} \int d\omega' [f_F(\omega') + f_B(\omega + \omega')]$$

$$\times A(\mathbf{k}', \omega') \operatorname{Im}\Gamma(\mathbf{k}+\mathbf{k}', \omega+\omega'),   (2.11)$$

where $f_F(x) = 1/(e^{x/T}+1)$ and $f_B(x) = 1/(e^{x/T}-1)$. The real part of Σ is obtained through the use of $\operatorname{Im}\Sigma$ in the Kramers-Kronig (KK) relation

$$\operatorname{Re}\Sigma(\mathbf{k}, \omega) = -\mathrm{p.v.}\int \frac{d\omega'}{\pi} \frac{\operatorname{Im}\Sigma(\mathbf{k}, \omega')}{\omega - \omega'},   (2.12)$$

where p.v. means the principal-value integral. The t matrix is

$$\Gamma(\mathbf{q}, \omega) = \frac{-V^2 \phi(\mathbf{q}, \omega)}{1 - V\phi(\mathbf{q}, \omega)},   (2.13)$$

where $\operatorname{Im}\phi(\mathbf{q}, \omega)$ is given by

$$\operatorname{Im}\phi(\mathbf{q}, \omega) = \pi \sum_{\mathbf{k}} \int d\omega' f_{\mathbf{k}}^2 \tanh\frac{\omega'}{2T} A(\mathbf{k}, \omega')$$

$$\times A(\mathbf{q}-\mathbf{k}, \omega-\omega'),   (2.14)$$

and the real part of $\phi(\mathbf{q}, \omega)$ is also obtained using the KK relation. The electron number is obtained through

$$\langle n \rangle/2 = \sum_{\mathbf{k}} \int d\omega A(\mathbf{k}, \omega) f_F(\omega),   (2.15)$$

and the spectral function must satisfy the sum rule

$$1 = \sum_{\mathbf{k}} \int d\omega A(\mathbf{k}, \omega).   (2.16)$$

This will be a check for the accuracy of the numerical results presented here.

In the actual calculation, the fast Fourier transformation is applied to accelerate the procedure.[30] The first Brillouin zone is divided into a 64×64 lattice and the frequency integration is replaced by a discrete sum in the range $-25t < \omega < 25t$, dividing it into 512 small intervals. As a consequence, the energy resolution is about $0.1t$, indicating the order of magnitude of the lowest temperature at which our calculations can be reliably carried out. When the relative difference between two successive iterations for $A(\mathbf{k}, \omega)$ is less than 0.01 at each $(\mathbf{k}, \omega)$, the iteration loop is terminated. As for the sum rule, it is systematically found to be satisfied within 1%. This value is the limitation for the accuracy of the present calculation, because the integral equation with a singular kernel is solved by replacing the integration procedure by a simple discrete summation.

C. s-d conversion

For a separable potential with d-wave symmetry, $f_{\mathbf{k}}$ is given by

$$f_{\mathbf{k}} = \cos k_x - \cos k_y.   (2.17)$$

In this case, due to the prefactor $f_{\mathbf{k}}^2$ in Eq. (2.11), Σ always vanishes along the lines $k_x = \pm k_y$, leading to a delta-function contribution in the spectral function. In order to avoid this singularity, a self-consistent calculation for the d-wave case was first attempted by imposing antiperiodic and periodic boundary conditions for the k_x and k_y directions, respectively. However, it was not always possible to obtain a converged self-consistent solution in this case. Actually, it was quite difficult to control such convergence even if the temperature T was slowly decreased from the high-temperature region in which a stable solution was obtained, or if the coupling V was adiabatically increased from the weak-coupling region.

This difficulty is caused by the fact that Σ becomes negligibly small in the region around $k_x \approx \pm k_y$ for the d-wave case, even if the strong-coupling value for V is set as high as $V = 8t$. If $\operatorname{Im}\Sigma$ becomes smaller that the energy resolution in the present calculation, which is about $0.1t$, the sharp peak structure in the spectral function around $k_x \approx \pm k_y$ is not correctly included in the self-consistent calculation. This leads to a spurious violation of the sum rule, indicating that technical problems appear in reaching a physically meaningful solution for d-wave symmetry at low temperatures.

In order to avoid this difficulty, a continuous change from s- to d-wave symmetry is here considered by introducing a mixing parameter α such that

$$f_{\mathbf{k}}^2 = (1-\alpha) + \alpha(\cos k_x - \cos k_y)^2.   (2.18)$$

Our calculations start at $\alpha = 0$, i.e., for the pure s-wave case, in which a stable solution can be obtained easily in the SCTMA. Then, α is gradually increased such that the d-wave case is approached. If a physical quantity for the

d-wave model is needed, an extrapolation is made by using the calculated results for the quantities of interest between $0 \leq \alpha < 1$.

Note that the momentum dependence of Σ is mainly determined by the prefactor $f_{\mathbf{k}}^2$. For $\alpha \neq 0$, $f_{\mathbf{k}}^2$ takes minimum values on the lines $k_x = \pm k_y$, indicating that the scattering amplitude becomes the weakest on these lines. Especially for $\alpha = 0$, i.e., the pure d-wave case, it vanishes on those lines. This corresponds to a tendency to the formation of nodes in the PG, which has been observed in ARPES experiments for underdoped HTSC. In this sense, α is not only a mathematical convenient quantity, but also a physical parameter to control the nodal behavior of the PG.

III. RESULTS

In this section, our results calculated with the use of the real-axis formalism are shown. Here the magnitude of the interaction V is fixed as $V = 8t$. As mentioned in Sec. I, ''holes'' in HTSC are treated as ''electrons'' in this paper. Thus the number density in the following discussion is related to the hole concentration in the real materials.

A. Case of $t' = 0$

Let us consider first the band structure with $\mathbf{k}^* = (0,0)$. In Fig. 2(a), the total density of states $\rho(\omega)$ is shown, given by $\rho(\omega) = \Sigma_{\mathbf{k}} A(\mathbf{k}, \omega)$. The whole curve for TDOS is not presented in this figure, because its shape at a larger scale is quite similar to the noninteracting case. At $\alpha = 0$, a gaplike feature at the Fermi level can be observed, although it is shallow. This result has been already reported in numerous previous papers using several techniques.[28] With the increase of α, the gap structure gradually becomes narrower and at the same time deeper. The TDOS extrapolated to $\alpha = 1$ using the results for the αs in the figure is not shown, because it becomes unphysically negative in some energy region. However, this is not a serious problem, because such a behavior is only an artifact due to the extrapolation using a small number of α results and it will disappear if α approaches unity very slowly and calculations with higher-energy resolution are performed. This problem is not present in the studies at $t' = 0$ in the next subsection. Thus this is a small complication that can be solved with more CPU and memory-intensive studies than reported here.

In order to understand the observed changes in the PG behavior with the increase of α, special attention must be given to the spectral function $A(\mathbf{k}, \omega)$. Let us first analyze the result at $\mathbf{k} = (0,0)$, shown in Fig. 2(b), in which two peaks are observed. The large peak above the Fermi level is due to the quasiparticle (QP) contribution, because if the interaction is gradually decreased, it continuously changes into the expected noninteracting δ-function peak. Thus here it will be called ''the QP peak.'' However, note that another structure can be observed below the Fermi level, although it has only a small weight. As will be discussed in the next subsection, this originates from the peak structure in Im Γ. In this sense, it can be called ''the resonant peak'' due to the formation of the bound pair.[11] When α is increased, the QP peak becomes sharper and the position of the resonant peak is shifted to the right side in Fig. 2(b), while the weight
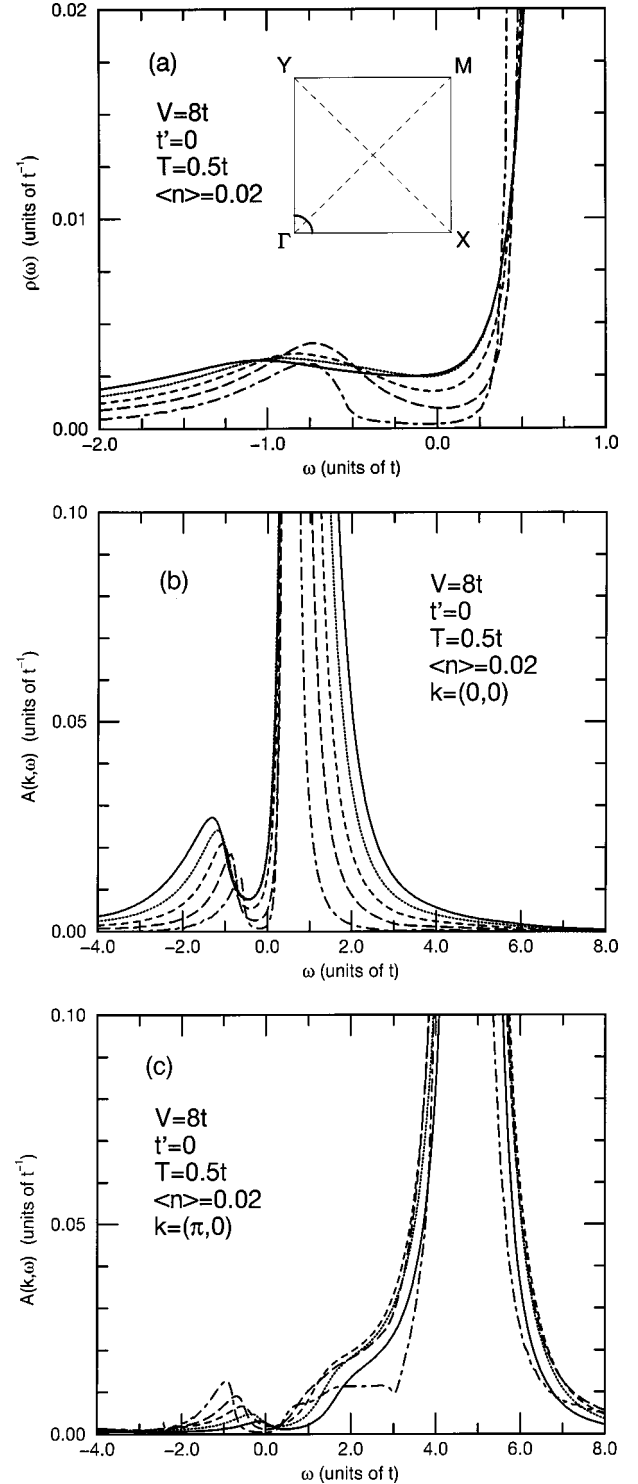

FIG. 2. (a) Total density of states (TDOS) for several values of α, the interpolating parameter between s- and d-wave models, in the case $V = 8t$, $t' = 0$, $T = 0.5t$, and $\langle n \rangle = 0.02$. The inset shows the Fermi line for this filling with $t' = 0$. The solid, dotted, dashed, long-dashed, and dot-dashed curves denote the TDOS results for $\alpha = 0, 0.2, 0.4, 0.6$, and 0.8, respectively. (b) The spectral function at $\mathbf{k} = (0,0)$. (c) The spectral function at $\mathbf{k} = (\pi, 0)$.

decreases. At $\alpha = 1$, the resonant peak will likely disappear and only the δ-function QP peak will occur, since the self-energy vanishes due to the prefactor $f_{\mathbf{k}}^2$ in Eq. (2.11).

Although the weight for the resonant peak in $A(\mathbf{k}, \omega)$ with $\mathbf{k} = (0,0)$ decreases with the increase of α, it is actually
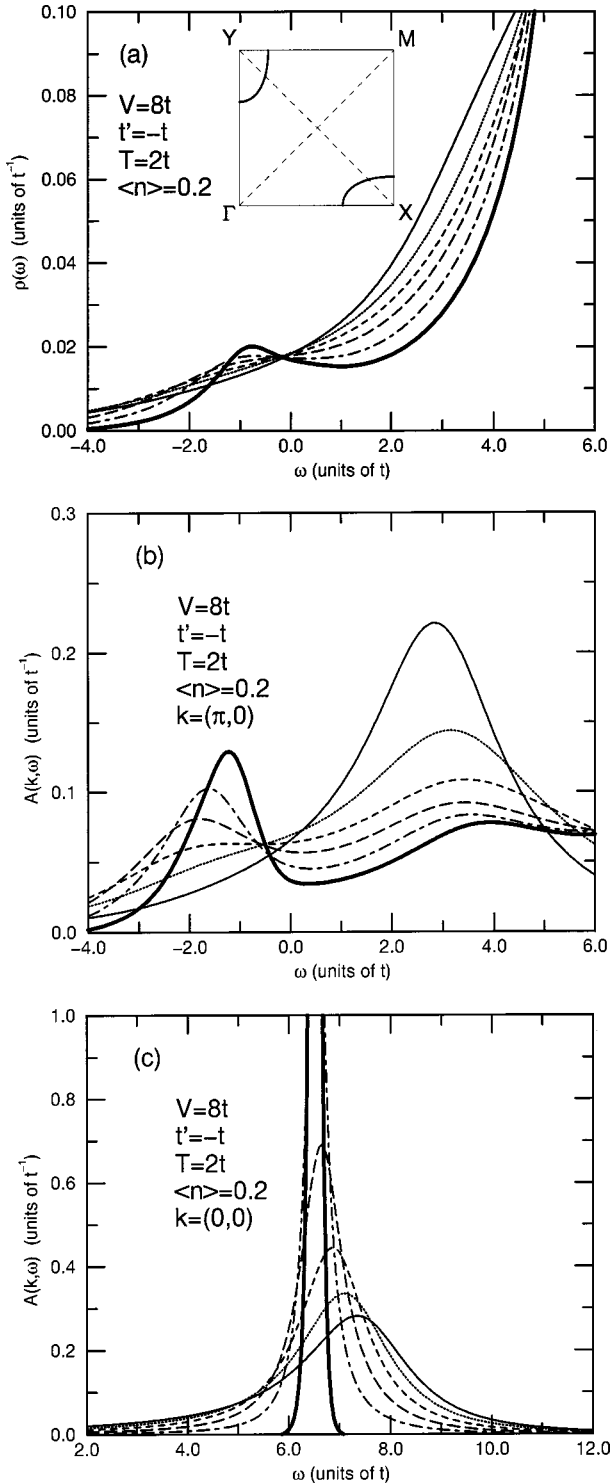
FIG. 3. (a) Total density of states (TDOS) for several values of α in the case of $V=8t$, $t'=-t$, $T=2.0t$, and $\langle n\rangle=0.2$. The inset shows the Fermi line for this filling with $t'=-t$. The solid, dotted, dashed, long-dashed, and dot-dashed curves denote the TDOS for $\alpha=0,0.2,0.4,0.6$, and 0.8, respectively. The thick solid curve is an extrapolated to $\alpha=1$ result from the available TDOS's in the interval $0\le\alpha<1$. (b) The spectral function at $\mathbf{k}=(\pi,0)$. (c) The spectral function at $\mathbf{k}=(0,0)$.

tween the positions of those QP peaks is about $4t$, namely, equal to $\varepsilon_{(\pi,0)}-\varepsilon_{(0,0)}$. It should be noted that another peak structure grows below the Fermi level with the increase of α. The position roughly agrees with the lower edge of the PG structure in the TDOS, suggesting that the PG structure for d wave originates from $A(\mathbf{k},\omega)$ around $\mathbf{k}=(\pi,0)$.

Let us summarize this subsection. Pseudogap features appear in the density of states both for s- and d-wave models, but its origin is quite different. For the s-wave case, this structure is mainly due to the preformed pair of electrons around the point $\mathbf{k}=\mathbf{k}^*=(0,0)$ at the bottom of the band. On the other hand, for the d-wave case, it originates from the pair of electrons at other $\mathbf{k}$-points, especially $\mathbf{k}=(\pi,0)$. In the case of strong attraction such as $V=8t$, those electrons can exploit the effect of the attractive interaction, in spite of the loss of the kinetic energy. In other words, this difference is due to the competition between the kinetic and the interaction effects.

B. Case of $t'\neq0$

From the result for $t'=0$, in order to obtain a large PG structure for d-wave symmetry, it is necessary to consider the band structure in which $\mathbf{k}^*$'s are located at $(\pm\pi,0)$ and $(0,\pm\pi)$. The reason is that electrons around $\mathbf{k}=\mathbf{k}^*$ can exploit the kinetic as well as the pairing energy due to the strong attractive interaction. As for a value of t', it is here typically chosen as $t'=-t$ but the results do not depend crucially on such a choice.

In the TDOS shown in Fig. 3(a), no structure around the Fermi level is observed for the s-wave case, but a peak appears below the Fermi level with the increase of α. It can be regarded as a sign of PG formation, but this interpretation becomes much clearer if $A(\mathbf{k},\omega)$ is investigated. In Fig. 3(b), the change of $A(\mathbf{k},\omega)$ at $\mathbf{k}=\mathbf{k}^*=(\pi,0)$ is depicted when α is increased. In the pure s-wave case, a large QP peak can be observed, but it is difficult to find a resonant peak below the Fermi level. On the other hand, when the d wave is approached by increasing α, the QP peak is gradually destroyed and the resonant peak grows strongly below the Fermi level. Then, the PG structure is much larger compared to that at $t'=0$. Note that in this case, the extrapolation for the TDOS at $\alpha=1$ is quite successful, contrary to what occurs at $t'=0$, because the large size of the PG allows us to perform the calculation at a high temperature such as $T=2t$, a situation in which the structure in the TDOS is smoother than at $t'=0$.

For the case $t'=-t$, weight transfer in $A(\mathbf{k},\omega)$ is observed with the increase of α, but it occurs between the QP and the resonant peaks at $\mathbf{k}=(\pi,0)$. In order to confirm this idea, $A(\mathbf{k},\omega)$ at $\mathbf{k}=(0,0)$ was studied as shown in Fig. 3(c). As expected, only the sharpening of the QP peak is observed as α is varied, because the strength of the attractive interaction at $\mathbf{k}=(0,0)$ becomes weak with the increase of α. Note that a finite width for the QP remains at $\alpha=1$, but it is only a numerical artifact. Actually at $t'=-t$, electrons around $\mathbf{k}=(0,0)$ do not take part in the PG formation even for the s-wave case. Since electrons around $\mathbf{k}=\mathbf{k}^*$ gain both the kinetic and potential energies, the PG structure is determined only by those electrons.

transfered to another $A(\mathbf{k},\omega)$ with $\mathbf{k}\neq(0,0)$. Then, let us next turn our attention to $A(\mathbf{k},\omega)$ with $\mathbf{k}=(\pi,0)$, shown in Fig. 2(c). In this case, a QP peak is also observed, but the position is higher than that at $\mathbf{k}=(0,0)$. The difference be-

IV. DISCUSSION

A. Energy scale for pseudogap

From the results in the previous section, in addition to the QP peak, a resonant peak below the Fermi level in $A(\mathbf{k}^*,\omega)$ has been observed, although its appearance depends on the value of t' and the symmetry of the pair interaction. These two peaks define the PG structure in $A(\mathbf{k}^*,\omega)$ and also in the TDOS, although in the latter it is often difficult to observe due to the smearing effects of the sum over momentum of the individual one-particle spectral functions. Based on these observations, in this paper the PG energy Δ_{PG} is defined by the width between the QP and the resonant peaks in $A(\mathbf{k}^*,\omega)$. Note that for $t'=0$ and $\alpha=1$, the weight for the resonant peak in $A(\mathbf{k}^*,\omega)$ will vanish, but in the limit of $\alpha \to 1$, its position approaches the lower peak of the PG structure.

In order to elucidate the physical meaning of our Δ_{PG}, the imaginary part of the self-energy is analyzed at $\mathbf{k}=\mathbf{k}^*$, because its structure has a direct effect on the spectral function, given by

$$A(\mathbf{k},\omega)$$
$$= -\frac{1}{\pi}\frac{\mathrm{Im}\,\Sigma(\mathbf{k},\omega)}{[\omega-(\varepsilon_{\mathbf{k}}-\mu)-\mathrm{Re}\,\Sigma(\mathbf{k},\omega)]^2+[\mathrm{Im}\,\Sigma(\mathbf{k},\omega)]^2}.$$
$$(4.1)$$

For an intuitive explanation, it is not convenient to analyze the full self-consistent solution for $\mathrm{Im}\,\Sigma(\mathbf{k},\omega)$. Rather, the essential information can be obtained by simply evaluating Eq. (2.11) replacing the renormalized Green's function G with the noninteracting Green's function G_0. Then, $A(\mathbf{k}',\omega)$ on the right-hand side of Eq. (2.11) becomes $\delta(\omega-\varepsilon_{\mathbf{k}'}+\mu)$ and $\mathrm{Im}\,\Gamma$ is obtained with the use of the p-p ladder diagrams composed of two G_0 lines. Furthermore, only the contribution from the preformed pair with momentum zero for the center of mass is considered. Namely, only $\mathrm{Im}\,\Gamma$ with $\mathbf{k}+\mathbf{k}'=0$ is taken into account in Eq. (2.11).

Due to the above simplifications, $\mathrm{Im}\,\Sigma$ at $\mathbf{k}=\mathbf{k}^*$ can be shown to be

$$\mathrm{Im}\,\Sigma(\mathbf{k}^*,\omega)\approx f_{\mathbf{k}^*}^2[f_{\mathrm{F}}(\varepsilon_{\mathbf{k}^*}-\mu)+f_{\mathrm{B}}(\omega+\varepsilon_{\mathbf{k}^*}-\mu)]$$
$$\times \mathrm{Im}\,\Gamma(\mathbf{0},\omega+\varepsilon_{\mathbf{k}^*}-\mu). \quad (4.2)$$

If it is assumed that $\mathrm{Im}\,\Gamma$ has a peak at $\omega=\Omega$, then $\mathrm{Im}\,\Sigma(\mathbf{k}^*,\omega)$ shows a peak structure around $\omega\approx\Omega-(\varepsilon_{\mathbf{k}^*}-\mu)$. Here the weight of the peak will not be discussed, but it will have a small finite value if the thermal factor is taken into account. Therefore in the spectral function at $\mathbf{k}=\mathbf{k}^*$, besides the sharp QP peak at $\omega=\varepsilon_{\mathbf{k}^*}-\mu$, another peak appears around $\omega\approx\Omega-(\varepsilon_{\mathbf{k}^*}-\mu)$ due to the peak-structure in $\mathrm{Im}\,\Sigma(\mathbf{k}^*,\omega)$, indicating that the size of the PG feature is given by $\Delta_{\mathrm{PG}}=|2(\varepsilon_{\mathbf{k}^*}-\mu)-\Omega|$ in this simple approximation.

Now let us estimate the value of Ω. Since Ω is the energy at which Γ acquires its maximum value, it can be obtained from the condition

$$1-V\,\mathrm{Re}\,\phi_0(\mathbf{0},\Omega)=0, \quad (4.3)$$

where ϕ_0 is the p-p ladder set with two G_0 lines, explicitly given by

$$\phi_0(\mathbf{q},\omega)=\sum_{\mathbf{k}} f_{\mathbf{k}}^2\frac{f_{\mathrm{F}}(\varepsilon_{\mathbf{k}}-\mu)-f_{\mathrm{F}}(-\varepsilon_{\mathbf{q}-\mathbf{k}}+\mu)}{\omega+i\eta-(\varepsilon_{\mathbf{q}-\mathbf{k}}+\varepsilon_{\mathbf{k}}-2\mu)}. \quad (4.4)$$

In the dilute case in which the chemical potential μ is situated below the lower band edge $\varepsilon_{\mathbf{k}^*}$ and in the temperature region for $T\lesssim\varepsilon_{\mathbf{k}^*}-\mu$, Eq. (4.3) reduces to

$$1+V\sum_{\mathbf{k}} f_{\mathbf{k}}^2\frac{1}{\Omega-2(\varepsilon_{\mathbf{k}}-\mu)}=0, \quad (4.5)$$

which is just the equation to obtain the binding energy Δ of the Cooper pair in the two-particle problem.[31] Since Δ is defined as the difference between the two-particle bound-state energy Ω and twice the one-particle energy $\varepsilon_{\mathbf{k}^*}-\mu$, it is given by

$$\Delta=2(\varepsilon_{\mathbf{k}^*}-\mu)-\Omega. \quad (4.6)$$

Then, from this analysis it is found that $\Delta_{\mathrm{PG}}=\Delta$, as intuitively expected.

B. Quantitative comparison between Δ and Δ_{PG}

Although the discussion in the previous subsection is too simple to address the fully renormalized self-consistent solution, the results reported in Sec. III will become more reasonable if the relevant energy scales are correctly addressed. In order to understand this, let us make a direct comparison between the analytic value for Δ and Δ_{PG} evaluated from the energy difference between the two peaks in $A(\mathbf{k}^*,\omega)$.

By solving Eqs. (4.5) and (4.6), the binding energy for the s- and d-wave cases with $t'=0$ and $t'=-t$ is obtained, which is shown in Fig. 4(a). In the strong-coupling region $V\gtrsim8t$, all curves are proportional to V. In the weak-coupling region, it is difficult to obtain an accurate value numerically, because the binding is exponentially small in this region. Especially, for the d-wave case with $t'=0$, it was not possible to obtain any finite value in a region of $V\lesssim7t$. However, when negative t' is introduced, the binding energy for d-wave pair is much enhanced, while the s-wave binding energy is not much affected by t'.

This result can be understood once again as caused by the competition between the band structure and the attractive interaction at $\mathbf{k}=\mathbf{k}^*$. For the s-wave case, since the attractive interaction is isotropic in momentum space, the V dependence of Δ is not so sensitive to the position of $\mathbf{k}^*$. However, for the d-wave symmetry, the situation is drastically different. For the band structure with $\mathbf{k}^*=(0,0)$, it is quite difficult for electrons around $\mathbf{k}=\mathbf{k}^*$ to form a pair, because the attraction does not work at $\mathbf{k}=\mathbf{k}^*$. Thus in the weak-coupling region the binding energy is vanishingly small. If V becomes as large as the bandwidth, $8t$, electron pairs at $\mathbf{k}\neq\mathbf{k}^*$ begin to affect the binding energy and the value of Δ becomes comparable to t. On the other hand, for the band structure with $\mathbf{k}^*=(\pi,0)$, electrons around $\mathbf{k}=\mathbf{k}^*$ easily form a pair because of the large strength of the attraction at that point. This sensitivity of the d-wave binding energy to the band structure is consistent with that of the d-wave PG observed in the spectral function.
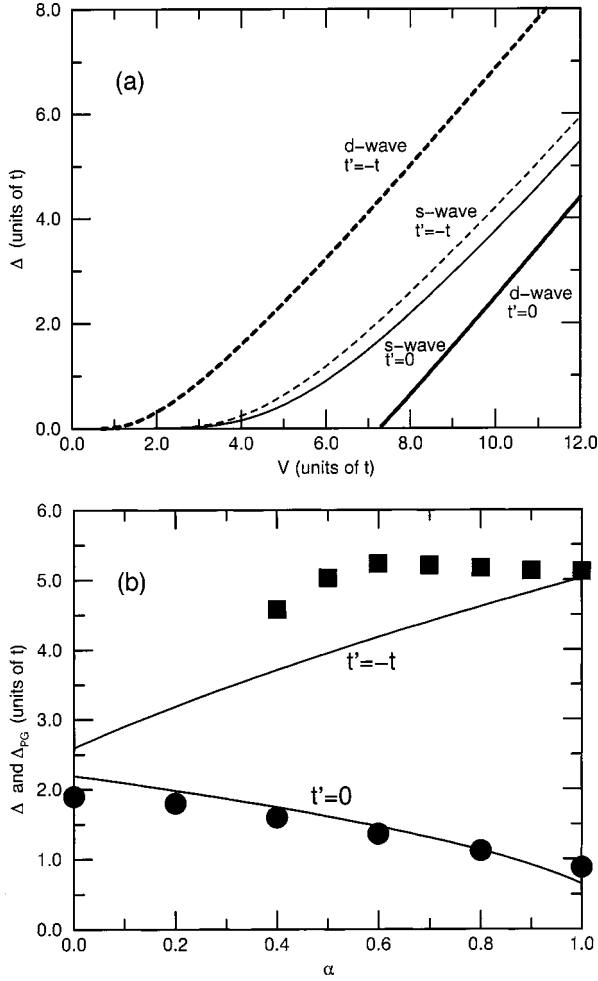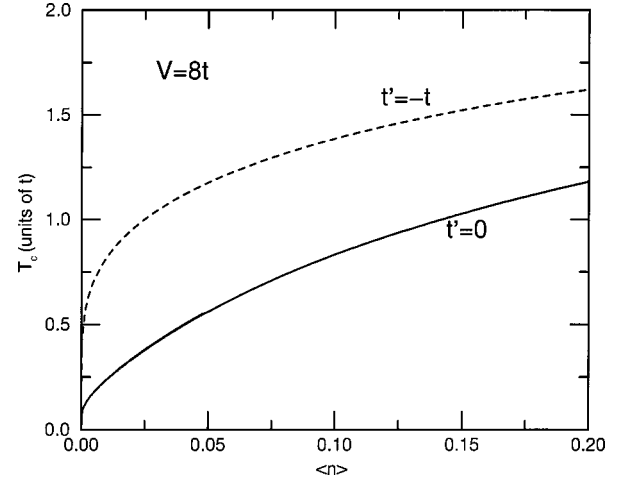
FIG. 5. Superconducting transition temperature in the mean-field approximation for d-wave pairing as a function of the electron number density for $t'=0$ and $t'=-t$ with $V=8t$.

than the superconducting transition temperature T_c. Otherwise, the results found in our work may be confused with the superconducting gap expected below T_c. It is necessary to check this assumption, but it is a very hard task to calculate the true value of T_c. Then, in order to provide an upper limit for T_c, the critical temperature is simply evaluated within the mean-field approximation. It is expected that the true T_c will be lower than the mean-field value T_c^{MF}, which is obtained from the well-known gap equation

$$1 = V \sum_{\mathbf{k}} f_{\mathbf{k}}^2 \frac{\tanh[(\varepsilon_{\mathbf{k}} - \mu)/(2T_c^{\mathrm{MF}})]}{\varepsilon_{\mathbf{k}} - \mu}. \qquad (5.1)$$

In Fig. 5, T_c^{MF} for d-wave pairing with $t'=0$ and $t'=-t$ is shown as a function of $\langle n \rangle$. For $t'=0$, the calculation for the spectral function shown in Sec. III has been done at $\langle n \rangle = 0.02$ and $T=0.5t$, and the point $(\langle n \rangle, T)=(0.02, 0.5)$ is located above the curve of T_c^{MF} in agreement with our assumption. Also for $t'=-t$, it is found from the figure that the temperature $T=2t$ used for $t' \neq 0$ is larger than T_c^{MF}, even at $\langle n \rangle = 0.2$. Clearly the temperatures analyzed in the present paper are above the superconducting critical temperature. Also note that Δ_{PG} for d-wave pairing is larger than T_c^{MF}. In particular, for the case of $t'=-t$, it is about three times larger than T_c^{MF}. This fact clearly suggests the appearance of a pseudogap temperature region, $T_c \lesssim T \lesssim \Delta_{\mathrm{PG}}$, for d-wave superconductors models.

As observed in Fig. 5, T_c^{MF} converges to zero in the limit $\langle n \rangle = 0$ in proportion to $\langle n \rangle^{\beta}$, where $\beta = 1/2$ in the BCS-like mean-field treatment. The true value of T_c is also expected to be zero in the limit $\langle n \rangle = 0$, but with $\beta > 1/2$ to keep the relation $T_c < T_c^{\mathrm{MF}}$. On the other hand, Δ_{PG} converges to the two-particle binding energy in the same limit. Thus in our scenario the PG region, $T_c \lesssim T \lesssim \Delta_{\mathrm{PG}}$, always exists in the dilute limit. However, the pairing symmetry of PG with the largest value of Δ_{PG} will depend on the kinetic term. In fact, the d-wave PG structure has been obtained for the band structure with $t'=-t$, while the s-wave PG has emerged for the case of $t'=0$. If the present analysis is performed for other band structures, it will be possible to put constraints on

FIG. 4. (a) Pair binding energy as a function of the interaction V, which is an analytic result obtained from the two-particle problem. (b) Pair binding energy as a function of α for $t'=0$ (upper solid curve) and $t'=-t$ (lower solid curve) with $V=8t$. The solid symbols indicate the PG energy Δ_{PG} estimated from the width between the QP and the resonant peak in the spectral function. The solid circle and square indicate Δ_{PG} for $t'=0$ and $t'=-t$, respectively. The results at $\alpha=1$ is obtained by the extrapolation from the results for $\alpha<1$.

Now let us compare our PG energy Δ_{PG} with Δ. In Fig. 4(b), those quantities are depicted as a function of α. Note that these Δ_{PG}'s are estimated from $A(\mathbf{k}^*, \omega)$'s in Figs. 2(b) and 3(b). In the region $\alpha<0.4$ for $t'=-t$, the values of Δ_{PG} are not shown, because the resonant peak could not be observed for the parameters used in Fig. 3(b). For the case of $t'=0$, Δ_{PG} traces the curve of the binding energy, though there is a small deviation between them. On the other hand, for the case of $t'=-t$, the deviation is larger particularly around $\alpha \approx 0.6$, but Δ_{PG} approaches Δ at the d-wave case. Thus, from our analysis, it is clear that the energy scale for the PG structure is simply the pair binding energy.

V. COMMENTS AND SUMMARY

In this paper, pseudogap features in a model for d-wave superconductivity have been observed. An important observation to start the discussion is that implicitly it has been assumed in the results reported thus far that Δ_{PG} is larger

the band structure of HTSC by considering under what circumstance a d-wave PG appears. However, in order to carry out such an analysis, it is necessary to treat a more realistic model with the nearest-neighbor attractive interaction including the competition among s-, d-, and p-wave attractions. This point will be discussed elsewhere.

Let us now briefly comment on the imaginary-axis calculation with the Padé approximation. Some attempts were made to obtain the PG structure in the imaginary-axis formalism directly for the d-wave symmetry, but it was difficult to observe it in our results. It might be possible to obtain it, if much more effort was made on the imaginary-axis calculations, particularly on the Padé approximation. However, when the s-d conversion trick is also applied to the imaginary-axis calculation, a clear sign of the PG just below the Fermi level can be easily observed. Although both results in the real- and imaginary-axis calculations do not agree perfectly with each other, the position of the peak in the imaginary-axis result is found to be located just at the lower edge of the PG structure obtained in the real-axis calculation. In the absence of the real-axis results, such a small signal of the PG structure may be missed, because it could be regarded as a spurious result due to the Padé approximation.

Finally, let us discuss the possible relation of our PG to that observed in the ARPES experiments as well as in previous theoretical works. In our result, the PG is characterized by the binding energy of the Cooper pair, which is of the order of t in our models except for a numerical factor when the magnitude of the interaction is comparable to the bandwidth, i.e., $8t$. If t is taken as a typical value for HTSC, it becomes of the order of a sizable fraction of eV, which is larger than the observed value in the ARPES experiments. However, from the viewpoint of the t-J model, which is expected to contain at least part of the essential physics for the underdoped HTSC, the effective hopping is renormalized to be of order J, not t, where $J(\sim 1000$ K$)$ is the AF exchange interaction between nearest-neighbor spins.[32] With this consideration the order of magnitude of our PG energy becomes more reasonable.

In some previous theoretical works, the energy scale for PG has been discussed. In the scenario of the PG formation due to the spinon pairing,[4] the characteristic energy is given by J on the basis of the t-J model. The interpretation of the PG is different from the present analysis, but the magnitude of the PG itself will be of the same order. On the other hand, in the framework due to the AF spin fluctuation,[5] the PG temperature is characterized by the spin fluctuation energy ω_{SF}.[5] Naively, ω_{SF}^{-1} denotes a time scale for which the nearest-neighbor spins can keep antiparallel directions. In the Heisenberg model with the AF coupling J, this time scale can be estimated as J^{-1}. Thus roughly the relation $\omega_{SF} \sim J$ holds, indicating that the energy scale for PG is again related to J. Of course, this is only a qualitative discussion and actually for the HTSC material, ω_{SF} has been estimated as about 10 meV from experimental results.[33] However, it is natural that the energy scale for PG can be always related to J, because any reasonable theory for HTSC must take the effect of the AF background into account to some extent.

In summary, the pseudogap structure has been investigated in the low-density region for the separable potential model with s- as well as d-wave symmetry. After special technical attention was given to particular features of the d-wave potential that make some of the calculations unstable, it has been revealed that the effect on the PG structure of the Cooper pair symmetry manifests in the change of the weight for the resonant peak at $A(\mathbf{k}^*, \omega)$. Moreover, it has been clearly shown that the energy scale for the PG structure is just the pair binding energy, which is certainly larger than T_c.

[1] H. Yasuoka, T. Imai, and T. Shimizu, in *Strong Correlation and Superconductivity*, edited by H. Fukuyama, S. Maekawa, and A. P. Malozemoff (Springer-Verlag, Berlin, 1989), p. 254; W. W. Warren, Jr., R. E. Walstedt, G. F. Brennert, R. J. Cava, R. Tycko, R. F. Bell, and G. Dabbagh, Phys. Rev. Lett. **62**, 1193 (1989); M. Takigawa, A. P. Reyes, P. C. Hammel, J. D. Thompson, R. H. Heffner, Z. Fisk, and K. C. Ott, Phys. Rev. B **43**, 247 (1991); H. Alloul, A. Mahajan, H. Casalta, and O. Klein, Phys. Rev. Lett. **70**, 1171 (1993).

[2] J. W. Loram, K. A. Mirza, J. R. Cooper, and W. Y. Liang, Phys. Rev. Lett. **71**, 1740 (1993).

[3] A. G. Loesser, Z.-X. Shen, D. S. Dessau, D. S. Marshall, C. H. Park, P. Fournier, and A. Kapitulnik, Science **273**, 325 (1996); J. M. Harris, Z.-X. Shen, P. J. White, D. S. Marshall, M. C. Schabel, J. N. Eckstein, and I. Bozovic, Phys. Rev. B **54**, 15 665 (1996); H. Ding, T. Yokoya, J. C. Campuzano, T. Takahashi, M. Randeria, M. R. Norman, T. Mochiku, K. Kadowaki, and J. Giapintzakis, Nature (London) **382**, 51 (1996); H. Ding, M. R. Norman, T. Yokoya, T. Takeuchi, M. Randeria, J. C. Campuzano, T. Takahashi, T. Mochiku, and K. Kadowaki, Phys. Rev. Lett. **78**, 2628 (1997).

[4] G. Kotliar and J. Liu, Phys. Rev. B **38**, 5142 (1988); H. Fukuyama, Prog. Theor. Phys. **108**, 287 (1992); P. A. Lee and X.-G. Wen, Phys. Rev. Lett. **78**, 4111 (1997).

[5] B. P. Stojkovic and D. Pines, Phys. Rev. B **56**, 11 931 (1997); A. V. Chubukov and J. Schmalian, *ibid.* **57**, 11 085 (1998); J. Schmalian, D. Pines, and B. Stojkovic, Phys. Rev. Lett. **80**, 3839 (1998).

[6] J. Ranninger and J.-M. Robin, Phys. Rev. B **56**, 8330 (1997).

[7] M. Randeria, N. Trivedi, A. Moreo, and R. T. Scalettar, Phys. Rev. Lett. **69**, 2001 (1992); C. Sa de Melo, M. Randeria, and J. R. Engelbrecht, *ibid.* **71**, 3202 (1993); N. Trivedi and M. Randeria, *ibid.* **75**, 312 (1995).

[8] V. Emery and S. Kivelson, Nature (London) **374**, 434 (1995).

[9] R. Micnas, M. H. Pedersen, S. Schafroth, T. Schneider, J. J. Rodríguez-Núüñez, and H. Beck, Phys. Rev. B **52**, 16 223 (1995).

[10] J. M. Singer, M. H. Pedersen, T. Schneider, H. Beck, and H.-G. Matuttis, Phys. Rev. B **54**, 1286 (1996).

[11] B. Jankó, J. Maly, and K. Levin, Phys. Rev. B **56**, 11 407 (1997); I. Kosztin, Q. Chen, B. Jankó, and K. Levin, *ibid.* **58**, 5936 (1998).

[12] V. B. Geshkenbein, L. B. Ioffe, A. I. Larkin, Phys. Rev. B **55**, 3173 (1997).

[13] J. Ranninger and J.-M. Robin, Phys. Rev. B **56**, 8330 (1997).

[14] D. J. Newman and Betty Ng, Phys. Rev. B **55**, 2792 (1997).

[15] O. Tchernyshyov, Phys. Rev. B **56**, 3372 (1997); **57**, 2728 (1998).

[16] Y.-M. Vilk, S. Allen, H. Touchette, S. Moukouri, L. Chen, and A.-M. S. Tremblay, J. Phys. Chem. Solids **59**, 1873 (1998).

[17] A. Sherman and M. Schreiber, Phys. Rev. B **55**, 712 (1997).

[18] M. Franz and A. J. Millis, Phys. Rev. B **58**, 14 572 (1998).

[19] Bumsoo Kyung, E. G. Klepfish, and P. E. Kornilovitch, Phys. Rev. Lett. **80**, 3109 (1998).

[20] M. Letz, J. Supercond. **12**, 61 (1999).

[21] Jan R. Engelbrecht, A. Nazarenko, M. Randeria, and E. Dagotto, Phys. Rev. B **57**, 13 406 (1998).

[22] B. C. den Hertog, Phys. Rev. B **60**, 559 (1999).

[23] T. Ichinomiya and K. Yamada, J. Phys. Soc. Jpn. **68**, 982 (1999).

[24] V. P. Gusynin, V. M. Loktev, and S. G. Sharapov, cond-mat/9811207 (unpublished).

[25] E. Dagotto, J. Riera, Y. C. Chen, A. Moreo, A. Nazarenko, F. Alcarez, and F. Ortolani, Phys. Rev. B **49**, 3548 (1994).

[26] A. Nazarenko, A. Moreo, E. Dagotto, and J. Riera, Phys. Rev. B **54**, 768 (1996), and references therein.

[27] L. P. Kadanoff and G. Baym, *Quantum Statistical Mechanics* (Benjamin, New York, 1962).

[28] M. Randeria, in *Proceedings of the International School of Physics "Enrico Fermi,"* Varenna, 1997, edited by G. Iadonisi and J. R. Schrieffer (IOS Press, Amsterdam, in press).

[29] H. Vidberg and J. Serene, J. Low Temp. Phys. **29**, 179 (1977).

[30] W. H. Press, S. A. Teukolsky, W. T. Vetterling, and B. P. Flannery, *Numerical Recipes* (University of Cambridge, New York, 1986), p. 490.

[31] J. R. Schrieffer, *Theory of Superconductivity* (Addison-Wesley, New York, 1988), p. 30.

[32] E. Dagotto, A. Nazarenko, and A. Moreo, Phys. Rev. Lett. **74**, 310 (1995); D. Duffy, A. Nazarenko, S. Haas, A. Moreo, J. Riera, and E. Dagotto, Phys. Rev. B **56**, 5597 (1997).

[33] V. Barzykin and D. Pines, Phys. Rev. B **52**, 13 585 (1995).